Geotextiles and Geomembranes xxx (xxxx) xxx

Contents lists available at ScienceDirect

Geotextiles and Geomembranes

journal homepage: www.elsevier.com/locate/geotexmem

Regular Paper

Importance of thickness reduction and squeeze-out Std-OIT loss for HDPE geomembrane fusion seams

William Francey [a], R. Kerry Rowe [b,c,*]

[a] GeoEngineering Centre at Queen's – RMC, Department of Civil Engineering, Queen's University, Kingston, K7L 3N6, Canada
[b] Barrington Batchelor Distinguished University, Geotechnical and Geoenvironmental Engineering, GeoEngineering Centre at Queen's – RMC, Kingston, K7L 3N6, Canada
[c] Department of Civil Engineering, Queen's University, Kingston, K7L 3N6, Canada

ARTICLE INFO

Keywords:
Geosynthetics
Geomembranes
Seams
Welds
Squeeze-out
Antioxidants
Std-OIT
HDPE
Thickness reduction
Quality assurance

ABSTRACT

The difference in seam squeeze-out antioxidant loss (in terms of standard oxidative induction time, Std-OIT loss) and thickness reduction are evaluated for three different 1.5 mm-thick high density polyethylene (HDPE) geomembranes (GMBs) seamed using a variety of welding parameters and two different wedge welders. Partial squeeze-out antioxidant loss was detected in seams created from each of the three materials examined, with the majority off loss occurring when seam thickness reductions fell between 0.4 mm and 0.8 mm. Seams with thickness reduction exceeding 0.8 mm were found to exhibit greater squeeze-out Std-OIT loss, with near full Std-OIT depletion for one material. Wedge welder size was found to influence this relationship, some seams created with the large wedge welder exhibiting a near full Std-OIT depletion from squeeze-out at approximately 0.6 mm thickness reduction. Variation in seaming pressure and high load melt index (HLMI) were found to shift the degree of thickness reduction a seam may experience for a given welding speed and temperature, with higher seaming pressure and HLMI values generally resulting in greater thickness reduction. Although, for a given welding speed, wedge temperature, and sheet temperature combination, changes in seaming pressure had a limited effect on squeeze-out Std-OIT loss. This paper provides a rational basis into defining a practical 1.5 mm fusion seam thickness reduction criteria based on limiting antioxidant loss within a seam's squeeze-out and also provides a framework for identifying potentially higher risk fusion seams for future research.

1. Introduction

High-density polyethylene (HDPE) Geomembranes (GMBs) are commonly used as a hydraulic barrier for the containment of fluids (Hsuan et al., 2008; Abdelaal et al., 2019; Abdelaal and Rowe 2019; Di Battista and Rowe 2020; Rowe et al., 2009; McWatters et al., 2020; Morsy and Rowe 2020; Li et al., 2021; Morsy et al., 2021; Tuomela et al., 2021). It is critical that they be designed considering how GMB performance affects overall system performance (Rowe 2011; Rowe and Yu 2019) and especially on how GMB affects leakage (Rowe 1988, 2005, 2012, 2020, 2018; Rowe and Booker 1995). This paper addresses an especially critical location in the system: fusion welds, of which there is usually more than approximatly1500 m/ha.

HDPE GMBs typically consist of 96–97.5% polyethylene resin, 2–3% carbon black, and 0.5–1.0% other additives such as antioxidants and stabilizers (Hsuan and Koerner 1998). These additives, most notably antioxidants, help retard thermo-oxidative degradation of the polymer that can occur during material manufacturing, installation, and aging processes during the GMBs service life (Hsuan and Koerner 1998; Rowe and Sangam 2002; Scheirs 2009). Split into two conceptual categories, primary and secondary antioxidants, each function by either trapping, deactivating, or preventing to production of free radical species. Antioxidants in both categories may be further divided into different chemical types, each with an effective temperature range and a more specific purpose in terms of hindering free radical production (Hsuan and Koerner 1998). For example, hindered amine light stabilizers (HALS) can function as both a primary or secondary antioxidant, and are often included within a GMB to help retard aging processes related to UV exposure (Hsuan and Koerner 1998; Rowe and Sangam 2002). Another group, referred to as phosphites, exhibits a larger effective temperature range in excess of 150 °C and are considered process stabilizers used to mitigate degradation that may occur during manufacturing or installation (Hsuan and Koerner 1998). Other groups display lower effective temperature ranges, such as HALS or thiosynergists (effective

* Corresponding author. Department of Civil Engineering, Queen's University, Kingston, K7L 3N6, Canada.
E-mail address: kerry.rowe@queensu.ca (R.K. Rowe).

https://doi.org/10.1016/j.geotexmem.2022.09.003
Received 17 February 2022; Received in revised form 10 August 2022; Accepted 11 September 2022

temperature range <200 °C).

During installation, geomembrane rolls are shipped to site and seamed in-situ to create a continuous barrier. Thermo-fusion techniques using a dual track wedge welder and/or extrusion gun are the most common used when seaming HDPE GMBs (Müller 2007; Scheirs 2009). Sheets of GMB being joined pass both sides of the wedge-shaped heating element and are subsequently forced together by two nip-rollers. Fig. 1 illustrates a typical weld cross-section following dual-track wedge welding. The structural components of the seam are referred to as weld zones and are the areas where the welding machines nip roller have forced the two sheets together after partial melting across the sheets thickness has occurred. Between the two weld zones is located an air channel, which is pressurized and used as a non-destructive testing method for seam quality. Towards the extremities of the seam are two heat affected zones (HAZ), which are areas with a thickness equal to that of the sheet and are potentially subjected to relatively high welding temperatures. These areas may have the potential to be partially depleted of antioxidants (Rowe and Shoaib 2017, 2018; Zhang et al., 2017; Rowe and Francey 2018), however the difference between post-seaming HAZ Std-OIT and virgin sheet values is not as great as that potentially observed in a seam's squeeze-out beads (Zhang et al., 2017). Lastly, two squeeze-out beads are located towards the seam extremities, situated between two corresponding HAZs. These areas are the result of molten polymer exiting the weld zone during seaming, where it collects and subsequently cools at the edges of the seam. This location was shown to exhibit the greatest degree of potential antioxidant depletion immediately post-seaming (Zhang et al., 2017), and as such, has been the primary focus of further investigation in this study.

Zhang et al. (2017) examined the change in index properties a geomembrane may experience immediately after being seamed using three different welding parameter combinations, designated "hot and slow" (HS), "standard" (S), and "cool and fast" (CF). Seams created under both HS and S conditions exhibited significant Std-OIT irregularities within the squeeze-out, yielding std-OIT values ranging from 10 to 190 min and 9–220 min, respectively. The resulting std-OIT curves displayed two peaks, one of which corresponding to a near full depletion in Std-OIT within the seam's squeeze-out. Although differences in squeeze-out std-OIT were documented for the three welds, limited change in index peel and shear tensile strength and break elongation was observed between them.

Rowe and Shoaib (2018), examined the depletion of antioxidants and mechanical properties for one weld immersed in a synthetic leachate solution. After approximately 48 months of immersion at 40 °C, 65 °C, 75 °C, and 85 °C, the seam's HAZ was found to deplete in both antioxidants and mechanical properties faster than the sheet, with seam shear elongation having depleted 2.2 times faster than the tensile properties of the sheet. However, Zhang et al. (2017) and Rowe and Shoaib (2018) only examined seams made from one geomembrane (different in the two cases) with a limited set of welding parameters, leaving one to consider how seam antioxidant depletion may change when comparing welds produced using different materials and a greater array of welding parameters.

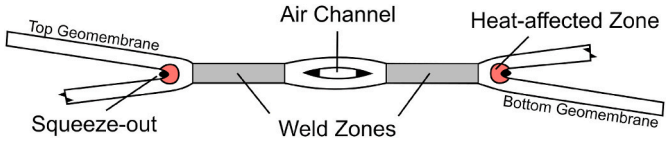

Fig. 1. Typical seam cross section produced by a dual-track wedge welder. The two weld zones are areas where sheet is forced together by the welding machine, providing the structural integrity for the seam. One center air channel, used as a non-destructive means of testing the seam though pressurization. Two heat-affected zones on either extremity of the seam. These areas exhibit the same thickness as the virgin sheet but are subjected to relatively high temperatures during seaming. Lastly, two squeeze-out beads on either extremity, in direct contact with two heat-affected zones.

Peggs (2019) assessed the implications of seam squeeze-out beads regarding craze formation and seam stress crack resistance (SCR) and concluded that a low Std-OIT squeeze-out bead may induce stress cracking within the HAZ area. Other work has examined the SCR of HDPE seams identifying this area as known point of weakness in the GMB barrier system as well as highlighted the roll seam squeeze-out geometry and extent can play on seam SCR (Halse et al., 1990; Hsuan 2000; Peggs and Carlson 1990; Peggs and Carlson 1990b; Peggs et al., 1990; Peggs et al., 2014; Francey and Rowe, 2022). Francey and Rowe (2022) examined SCR samples taken within the first 1 m of a field seamed HDPE dual-track wedge weld that contained a discontinuity within the squeeze-out bead along the axis parallel to the seam direction. Moreover, the squeeze-out bead itself was adhered to the bottom geomembrane sheet, allowing tensile load to be transferred along the squeeze-out bead when the seam was loaded in tension. This seam, although passing current GRI-GM19 peel-shear test strength-ductility criteria (ASTM D 6392), was found to have an un-notched seam SCR test value less than that of the virgin notched sheet (660 h for the un-notched seam, vs 1078 ± 83hr for the notched sheet), highlighting the importance of squeeze-out regarding seam SCR. In other work, the HAZ/squeeze-out area was found to be an area on increased strain concentration due to seam rotation when loaded in tension (Giroud et al., 1995; Kavazanjian et al., 2017), suggesting this area as the critical area with respect to non-indentation tensile strains. Thus, the squeeze-out is a particularly important feature of a weld that can act as a strain magnifier, a locations for potentially increased SCR susceptibility, alongside the potential antioxidant depletion within a seam squeeze-out bead and its adherence to the sheet, have prompted further examination of seam squeeze-out Std-OIT depletion. The identification of physical characteristics or undesirable welding parameters combinations affecting seam squeeze-out Std-OIT will provide CQA personnel greater confidence in the long-term performance of HDPE fusion seams and provide researchers insight into selecting "higher-risk" seams regarding long-term performance testing. The objectives of this paper are to:

1. Examine the effect of different welding parameters on seam thickness reduction and seam rippling for three distinctly different HDPE GMB formulations.
2. Identify potential welding parameters combinations negatively impacting seam squeeze-out Std-OIT.
3. Identify an acceptable seam thickness reduction range based on a range of welding parameter combinations and material HLMI values in order to mitigate potential squeeze-out antioxidant depletion.

2. Materials and methods

2.1. Materials

Three 1.5 mm HDPE GMBs were selected for this study based on their varying characteristics and index properties (Table 1). The first material, referred to as MwA-15, was a flat die HDPE GMB suspected to contained HALS and is marketed as an easily welded GMB, possibly attributed to its high, high load melt index (HLMI = 21.5 g/10 min) aiding in squeeze-out movement during welding. The second product, MyE-15, was a blown-film HDPE GMB that is suspected to contain HALS, but has a lower HLMI (14 g/10 min) than MwA-15. Lastly, MxA-15, was a blow-film HDPE geomembrane with an intermediate HLMI (19.7 g/10 min) manufactured in 2005 with no HALS (Ewais et al., 2014; Abdelaal and Rowe 2015) was selected because of its long storage-life and low post-manufacturing HP-OIT make it an interesting selection to examine the effect of seaming on partially aged GMBs with relatively less sophisticated antioxidant packages (potentially analogous to older geomembranes in service for the past 15 years). MxA-15's Std-OIT value at the time of testing had decreased to 87 ± 4 min, approximately 50% of its initial post-manufacturing value. This value is notably below the

Table 1
Index properties at the time of testing for the three geomembranes examined, MwA-15, MxA-15, and MyE-15.

Properties	Method	Unit	GMB1	GMB2	GMB3
Nominal thickness	ASTM D 5199	mm	1.5	1.5	1.5
GMB designation			MwA-15	MxA-15	MyE-15
Manufacturing date			2011	2005	2012
Manufacturing technique			Flat die	Blown film	Blown film
Standard oxidative induction time (Std-OIT)	ASTM D 3895	min	164 ± 5	87 ± 4	161 ± 1
High-pressure oxidative induction time (HP-OIT)	ASTM D 5885	min	1321 ± 12	260 ± 10	1300 ± 100
Suspected HALS			Yes	No	Yes
HLMI (21.6 kg/ 190 °C)	ASTM D 1238	g/10 min	21.5 ± 0.2	19.7 ± 0.4	14.0 ± 0.1
Stress Crack Resistance (SCR)	ASTM D 5397	hours	1078 ± 83	529 ± 85	13000 ± 1300
Tensile yield strength (MD)	ASTM D 6693 Type (IV)	kN/m	29.6 ± 0.5	29.3 ± 0.8	29.3 ± 1.0
Tensile yield strain (MD)		%	19.7 ± 0.3	19.4 ± 0.5	20.0 ± 0.4
Tensile break strength (MD)		kN/m	46.4 ± 0.3	38.9 ± .12.9	49.1 ± 6.5
Tensile break strain (MD)		%	760 ± 13.8	760 ± 84.0	720 ± 84

current GRI-GM13 guidelines of an acceptable Std-OIT of 100 min, meaning this product, as per GRI-GM13, is no longer suitable for use in a new installation at the time of testing but that was due to depletion over time as would happen in the field before a new panel in a new connecting cell was welded to it.

2.2. Seaming procedure

Seams were prepared using both a Demtech Pro Series wedge welder and a Leister G7 wedge welder, with corresponding heat element wedge lengths of ~80 mm and ~130 mm, respectively; referred to generically herein as WW80 and WW130. Welds were produced by an experienced geomembrane installer in both field and laboratory environments. Welding machine parameters were set to the desired welding speed, welding temperature, and pressure combinations and allowed to equilibrate prior to seaming. Ambient temperature conditions, and ultimately the sheet temperature at the time of welding, were controlled in three different ways. Warm welds were conducted in the field at Queens University's Environmental Liner Test Site (QUELTS II) and was exposed to midday sun with a sheet temperature equilibrated to 65 ± 5 °C prior to seaming. After welding, warm welds were then left for several hours under direct sun exposure to cool down, and later transported to the laboratory and stored at 21 °C before testing. 21 °C seams were welded in laboratory from sheet left to equilibrate to laboratory conditions for a minimum of 24 h prior to seaming. Lastly, sub-zero welds were created in an environmental chamber set to −27 ± 2 °C from GMB sheet left to condition for a minimum of 24 h. In all cases, prior to welding, sheet samples were wiped down with a cleaning rag to ensure dust or ice crystals from water vapor in the air were absent on sheets surfaces. Seams were all stored to equilibrate with ambient temperature conditions (21 °C) for at least 24 h post-seaming to allow equilibration with ambient conditions prior to the removal of specimens and subsequent testing procedures.

2.3. Weld thickness reduction

Weld thickness reduction can provide a preliminary indication of weld mechanical strength and any potential overheating that may have occurred during welding (Müller 2007; Scheirs 2009). In general, the greater the thickness reduction of a seam weld track the greater the heat and/or nip roller pressure used during seaming. It is hypothesized that excessive thickness reduction likely increases stress concentrations along the edge of the weld zone, as well indicates an increased likelihood that antioxidant depleted melt, in the form of squeeze-out, has migrated from the weld zone towards the HAZ, potentially having implications in long-term SCR performance. Conversely, too little a thickness reduction may serve as an indication of inadequate bonding within the seams weld zone, leading to peel test failure and weld separation. Weld thickness reduction is defined as the sum of the thicknesses of both the top and bottom GMB, or combined thickness of the two sheets to be welded, minus the thickness of the weld zone (Equation (1)) (Müller 2007; Scheirs 2009).

$$t_r = (t_t + t_b) - t_w \quad (1)$$

where t_r is the weld thickness reduction, t_w is the thickness of the weld track, and t_t and t_b are the thickness of the top and bottom sheet, respectively. Weld thickness reduction measurements were taken for all seams examined. Three thickness measurements were taken from both the inside and outside weld tracks using calipers for a total of six measurements. The average of those six was then used in calculating thickness reduction, with error being the standard deviation of those six samples. All thickness measurements were taken at the midpoint for each respective weld track, as the two opposing faces of a weld track may not always be perfectly parallel. It has been suggested that thickness reduction be reduced to an acceptable range, with certain regulatory bodies implementing their own guidelines on acceptable thickness reduction values. For example, the German DVS-2225-4 standard currently limits thickness reduction to 0.2–0.8 mm for a 2.5 mm HDPE GMB, with a 2.5 mm thickness being the minimum acceptable thickness GMB used in landfill applications in Germany. DVS 2225-3 allows the use of 1.5 mm GMBs for groundwater protection where it specifies that the thickness reduction fall between 0.2 and 0.6 mm for HDPE GMBs less than 2.0 mm. The results reported herein will examine the data in the context of these ranges as well as identify if changes in behavior occur within different thickness reduction ranges not specified within the DVS 2225-3 standard.

2.4. Oxidative induction time (OIT) testing

Standard oxidative induction time (Std-OIT) tests were used to assess the degree of antioxidant depletion on both sheet materials and seams post welding. This index test (ASTM D3895) has been used extensively for monitoring the depletion of antioxidants in GMBs during aging (Hsuan and Koerner, 1998; Rowe and Sangam, 2002; Rowe et al., 2009; Abdelaal et al., 2014; Morsy and Rowe 2020; Li et al., 2021; Morsy et al., 2021), as well as identifying antioxidant loss in GMB seam squeeze-out and HAZs (Rowe and Shoaib 2017, 2018; Zhang et al., 2017). Std-OIT tests were conducted using a TA instrument Q2000 differential scanning calorimeter (DSC) following ASTM D3895.

Examples of Std-OIT curves for a HDPE GMB sheet and seam squeeze-out are shown in Fig. 2. Irregularities were found within the thermograms of squeeze-out sections, consistent with the findings of Zhang et al., (2017). Much like Zhang et al. (2017), multiple peaks and ultimately different onset times can be identified within some squeeze-out Std-OIT thermograms. However, as the clear presence of an exothermic reaction occurs at the first peak and that Std-OIT values are

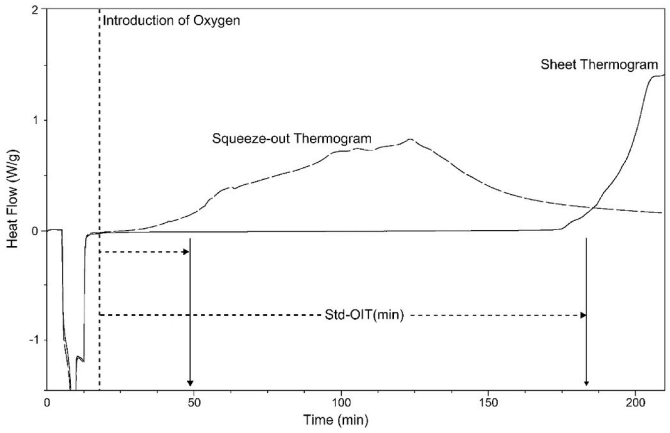

Fig. 2. Std-OIT thermogram examination for seam squeeze-out and sheet material. Values for both seam squeeze-out and sheet material were recorded at the onset of the first exothermic peak present within the thermogram. Irregularities and multiple peak were detected within squeeze-out samples, however, a clear initial peak was still present, particularly in relatively high heat applied seamed samples.

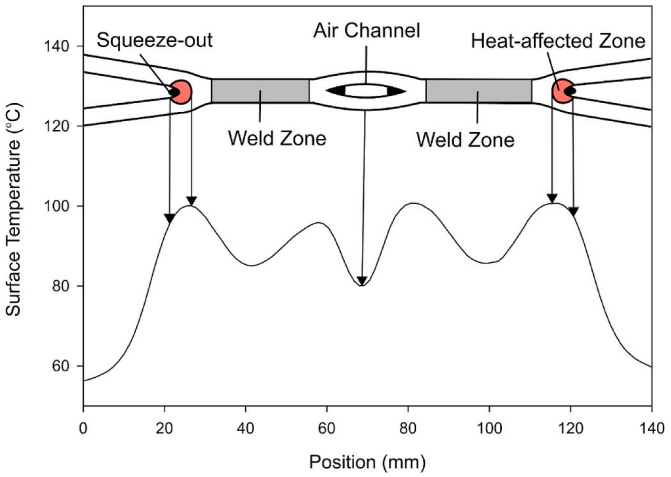

Fig. 3. Variation in geomembrane surface temperature or an MwA-15 seam created at a sheet temperature of 65 °C, with a corresponding welding temperatures and speed of 460 °C and 1.8 m/min, respectively. Peak temperatures observed were highest around the outside heat-affect zone areas, as the movement of molten polymer from the weld zone during the application of seaming pressure transferred heat towards the extremities of the seam.

often taken at the initial peak for sheet material specimens, this paper will focus primarily on reporting the time until initial peak values for squeeze-out Std-OIT. Moreover, both the initial peak and secondary peaks are often found to occur much sooner than the virgin sheet onset, suggesting substantial antioxidant depletion had occurred within many of the squeeze-out specimens examined. Many of the seam squeeze-out specimens, particularly those with higher thickness reductions, exhibited a singular exothermic peak corresponding to low Std-OIT times (e.g., squeeze-out thermogram in Fig. 2). Suggesting that near full depletion in antioxidants could occur during welding for the materials examined. Hence, samples that exhibited irregularities where analyzed based on the first peak time, as these irregularities within the exotherm were considered an important indicator of antioxidant depletion which had the potential to reduce to a near zero Std-OIT value upon greater heat addition during seaming.

3. Results

3.1. Examination of Seam thermal history

To gain insight into differences in peak weld zone and HAZ temperature, as well as the movement of molten polymer within the seams weld zone, surface temperature at the time of welding was monitored for one seam created at a sheet temperature of 65 °C. GMB seam surface temperature was monitored using a FLIR SC660 thermal imaging camera displaying surface temperatures to an accuracy of ± 1 °C. Wedge temperature was set to 460 °C with a welding speed of 1.8 m/min for the WW80 wedge welder. Temperature recording started the moment the welding machine had begun seaming and ended 180 s after the nip rollers had passed.

Fig. 3 illustrates the distribution of surface temperatures approximately 15 s after nip roller passed and represents the distribution of peak temperatures that occurred over the 180 s recording duration. Thermal imaging showed that peak temperatures occurred within the HAZs on both the inside and outside edge of the weld zone, where surface temperatures reached approximately 100 °C. Weld zone surface temperatures were found to vary between approximately 85 °C and 90 °C and were notably cooler than those of the inside and outside HAZs until approximately 130 s of cooling had elapsed, at which point weld zone surface temperatures remained higher than those of the HAZs at temperatures <100 °C. The observed distribution in temperature is hypothesized to be the result of molten polymer migration from the weld zones towards the HAZs after nip roller passing, where material in direct contact with the heating wedge is forced towards the extremities of the weld through the application of seaming stress. This suggests that a large proportion of the heat transferred to the HAZs came from the movement of molten polymer in the form of squeeze-out, rather than direct contact with the hot wedge and conduction through the sheet.

The selection of welding parameters dictated the amount squeeze-out. The squeeze-out was found to pool alongside the HAZ area increasing the HAZs temperature, monitoring index properties (e.g., Std-OIT) of the squeeze-out may provide insight into the likelihood of any potential HAZ degradation. It is hypothesized that greater squeeze-out degradation likely indicates a greater likelihood of HAZ degradation. Degradation of the HAZ may also only occur along its outer surface (i.e. where the squeeze-out has pooled), potential making it difficult to obtain an accurate Std-OIT value for comparison with the sheet as the proportion of material degraded may be too small for accurate Std-OIT testing. This is potentially shown in the partially degraded, but near sheet equivalent, HAZ Std-OIT values recorded in the literature (Rowe and Shoaib 2017; Zhang et al., 2017; Rowe and Francey 2018). It is hypothesized that in these cases heat transfer from the squeeze-out has degraded the HAZ surface, yielding an observable difference in Std-OIT compared to the sheet, although that portion of a HAZ Std-OIT specimen affected is unknown.

Surface temperature measurements of a HDPE GMB seam showed higher peak temperatures within the seams HAZ region than within the weld zone region. This suggests that molten polymer migration, in the form of squeeze-out, may be the primary factor contributing heat to a seam HAZ during seaming. Monitoring squeeze-out may provide a good indication of the overall heat added to the seam as high thickness reduction within the weld zone (i.e. removal of molten material in the form of squeeze-out) effectively reduces the amount of potentially degraded material from this zone as it pools towards the extremities of the weld. Thus, Std-OIT testing of a seams squeeze-out bead can provide a better indication (than a seam HAZ or weld zones) of the heat added to a GMB seam and the potential of antioxidant loss for a given set of welding parameters and materials.

3.2. Weld thickness variation

3.2.1. Effect of welding speed at 400 °C

Fig. 4a and b illustrate the magnitude change in weld thickness reduction over a range of welding speeds for both the WW130 and

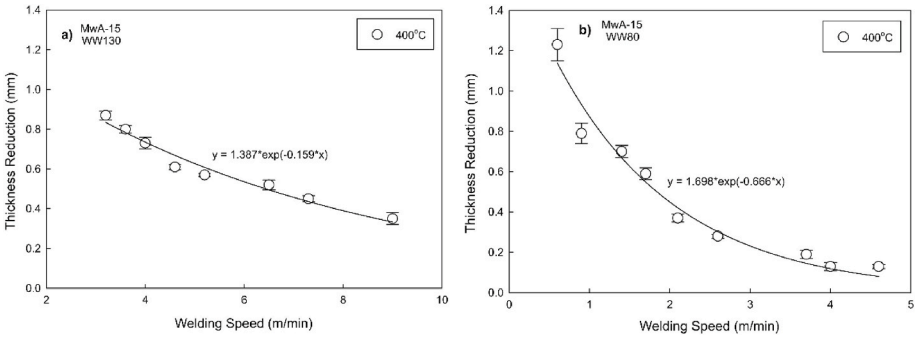

Fig. 4. Variation in seam thickness reduction (y) with changing speed (x) for WW130 and WW80 both seam created with a 21 °C sheet temperature, a 400 °C welding temperature and manufacturer recommended seaming force. Exponential curve fitting yielded R^2 of 0.96 for both WW130 and WW80.

WW80 wedge welders set to 400 °C conducted at a 21 °C sheet temperature. When sheet and wedge welding temperature is held constant, change in weld thickness reduction per unit change in welding speed was found to behave non-linearly, with a decrease in welding speed resulting in increased thickness reduction. This relationship progressed until weld thickness reduction was too high to provide support for the self-propelled welding machine's nip rollers, resulting in what is referred to as a "burn out" or "burn through" failure (Scheirs 2009). During a burn out failure the machine remains stationary as the nip rollers continue to rotate, unsuccessfully gripping to partially molten material and ultimately leading to the hot wedge burning through the sheet material. These burn outs are undesirable as they represent points of overheating along a continuous fusion seam and require further work to both prep for pressure CQA testing and require repair using a patch and extrusion welder. Furthermore, the extrusion welds necessary for repair are thought to be more prone to stress cracking failures than fusion welds, meaning limiting their use is advantageous to the liner systems integrity (Peggs and Carlson 1990b; Scheirs 2009).

Fitting an exponential curve to the thickness reduction/welding speed plots yielded a reasonable fit for both wedge welders examined, with an R^2 of 0.96 for both the WW130 and WW80. Conceptually, if one where to continually increase the welding speed infinitely the amount of thickness reduction would level off at 0 mm, as the amount of heat added to the weld further decreases with increasing speed. This leveling off would in turn result in non-linear behavior similar to that observed in Fig. 4. Conversely, if one progressively decreases the welding speed, effectively increasing the amount of heat added to the weld, the resulting thickness reduction increases until a point where burn out failure occurs. This implies that there is a threshold welding speed for a given set of weld temperature and pressure settings, beyond which any further reduction in welding speed would only result in burn outs and no continuous weld track.

Fig. 4a and b shows seams at speeds that produce viable welds prior to a burn out failure occurring. This corresponds to a minimum welding speed of approximately 3.25 m/min and 0.6 m/min for the WW130 and WW80 wedge welders, respectively. Beyond this point a burn out failure was achieved, although, not included in the exponential curve fitting. This is due to the significant rippling along the weld track around the burn out area making thickness reduction measurements difficult to obtain and potentially misleading, as the machine is stationary resulting in non-equilibrium thickness reduction values. Thus, burn out threshold welding speeds for the two cases examined where taken at the next highest speed which produced a viable weld. These minimum welding speeds translated to a burn out thickness reduction threshold (i.e., maximum thickness reduction prior to burn out) of approximately 0.87 mm and 1.23 mm for the WW130 and WW80 wedge welder, respectively. The difference in thickness reduction for a given speed between the two welders is considered to be the result of increased heat transfer for the larger WW130 compared to WW80. The manufacturer recommended welding speed of 7.9 m/min (26 ft/min) and seaming force of 1250 N for the WW130 produced a weld thickness reduction of approximately 0.4 mm, a value within the DVS 2225-3 thickness reduction range. While the WW80 produced seams with a thickness reduction of 0.4 mm at a welding speed of approximately 2 m/min. Indicating that for a given welding temperature and desired thickness reduction, the larger WW130 wedge welder can produce comparable seams at a much faster rate than the WW80.

3.2.2. *Effect of wedge temperature (352 °C, 400 °C, 460 °C) and welding speed*

To assess the effect of wedge temperature on the degree of thickness reduction two other welding temperatures were examined for the WW130 wedge welder (352 °C and 460 °C) using the same manufacturer recommended seaming force of 1250 N at a 21 °C sheet temperature. These temperatures are above and below the manufacturer recommended 1.5 mm HDPE GMB welding temperature of 400 °C for this machine. Fig. 5 shows the exponential curve fit for the 352 °C, 400 °C and 460 °C series of welds, with all three fitting reasonably well with corresponding R^2 values of 0.97, 0.96, and 0.98 for the 352 °C, 400 °C and 460 °C seam series, respectively. A vertical shift in thickness reduction is present between each of the series, where higher welding temperatures produce a greater degree of weld thickness reduction for a given welding speed. Table 2 outlines the interpolated welding speed and thickness reduction thresholds for each of the seaming temperatures and wedge welders taken from exponential curve fitting. The burn out welding speed threshold occurred at different welding speeds for the

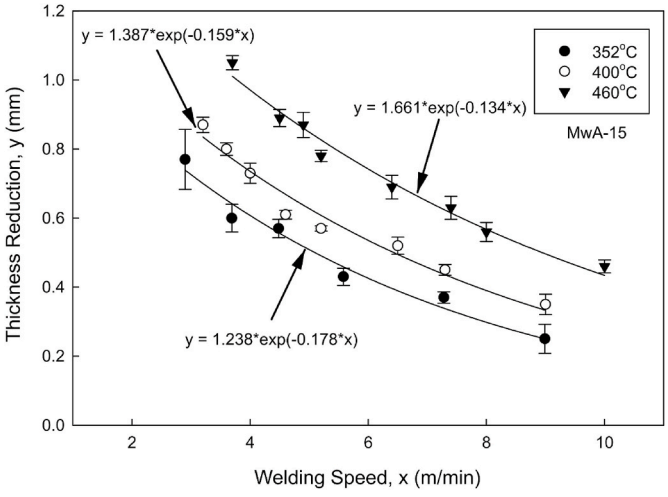

Fig. 5. Variation in MwA-15 seam thickness reduction (y) with changing welding speed (x) for three seam series created using WW130 at welding temperatures of 352 °C, 400 °C, and 460 °C. Seaming pressure and surface temperature at the time of welding for all three series was set to 1250N and 21 °C, respectively.

Table 2
Thickness Reduction and welding speed thresholds for the 4 seam series examined. Burn-out threshold represents the minimum welding speed which produced a viable weld prior to burn-out failure, while 0.2 mm and 0.6 mm t_r thresholds represent the speeds that produced welds adhering to the upper and lower limits of DVS 2225-3. The difference between these thresholds indicate the range of speeds which produce suitable welds based on DVS 2225-3, with WWW130 460°C exhibiting the greatest range of acceptable welding speeds based on thickness reduction.

Seam Series	Burn-out t_r Threshold (mm)	Burn-out Welding Speed Threshold (m/min)	0.2 mm t_r Welding Speed Threshold[a] (m/min)	0.6 mm t_r Welding Speed Threshold[a] (m/min)	Difference Between t_r Threshold Speed Values[a] (m/min)
WW130 352 °C	0.77	2.9	10.2	4.1	6.2
WW130 400 °C	0.87	3.2	12.2	5.3	6.9
WW130 460 °C	1.05	3.7	15.8	7.6	8.2
WW80 400 °C	1.23	0.6	3.2	1.6	1.6

[a] Taken from exponential curve fitting.

three WW130 cases examined (approximately 2.9 m/min, 3.2 m/min, and 3.7 m/min for the 352 °C, 400 °C and 460 °C series, respectively), while the amount of thickness reduction necessary to produce a burn out was less at lower welding temperatures (approximately 0.77 mm, 0.87 mm, and 1.05 mm for the 352 °C, 400 °C and 460 °C series, respectively). If one were to consider the observed thickness reduction change with regards to the German DVS 2225-3 standard on weld thickness reduction, where 0.2–0.6 mm reduction for a 1.5 mm HDPE GMB is acceptable, the actual range of speeds that produce acceptable thickness reductions was less for lower welding temperatures than higher ones. For example, speeds from 4.1 m/min – 10.2 m/min for the 352 °C series produced welds with an acceptable thickness reduction, while the 460 °C series exhibited acceptable thickness reductions from 7.6 m/min – 15.8 m/min. Moreover, both the range of acceptable welding speeds and the speeds required for 0.2 mm thickness reduction were found to be notably higher for WW130 than that of WW80 (Table 2). The relatively higher speeds that can be utilized with WW130, compared to WW80, are attributed to increased wedge size and greater heat transfer to the sheet. This suggests that a larger wedge welder will provide faster installation for a given thickness reduction seam and that there is more flexibility in welding speed selection with WW130 given the increased range of speeds producing thickness reductions from 0.2 mm to 0.6 mm.

Weld thickness reduction was found to increase with increasing wedge temperature, wedge length, and decreasing welding speed. The relationship between welding speed and thickness reduction was found to be non-linear and with a unit decrease in welding speed resulting in a greater unit thickness reduction for lower welding speeds than higher ones. This suggesting that care should be taken when changing welding speed when thickness reductions are high, especially when rapid changes solar insolation and sheet temperature are expected. Minimum welding speeds prior to burn out failure were greater for seams produced using higher wedge temperatures, with a corresponding minimum thickness reduction prior to burn out failure of ~0.8 mm (352 °C WW130 series). Thus, from a conservative burn out mitigation perspective, thickness reductions in 1.5 mm HDPE GMB seams should be kept to <0.8 mm.

3.3. Squeeze-out Std-OIT depletion

Squeeze-out Std-OIT antioxidant depletion was measured for both the WW130 and WW80 400 °C weld series. Like that reported by Zhang et al., (2017), in some cases, material morphological and additive heterogeneity within the squeeze-out produced an average Std-OIT with a high range in recorded values. Fig. 6a and b displays squeeze-out Std-OIT in relation to seam thickness reduction for both 400 °C weld series, with error bars representing the range of recorded values (n = 3). Both welding machines exhibited similar behavior with respect to Std-OIT loss at 400 °C, where an initial, seemingly linear, decrease in Std-OIT with decreasing welding speed progresses until a critical welding speed was reached. Once the critical welding speed was reached, Std-OIT variation within the squeeze-out significantly increased and the mean value started to rapidly decrease to a potentially residual value of approximately 20 min. Once past the Std-OIT the transition point, approximately 5.2 m/min and 0.9 m/min for the WW130 and WW80 welders respectively, a clear change in the shape of the weld track of the seams was observed. Fig. 7 illustrates this change and the development of 'ripples' along the seams two weld tracks. This observation is a known qualitative indication of seam overheating and has been discussed in the literature (Scheirs 2009; Francey and Rowe, 2022), although the relationship between weld track rippling and squeeze-out Std-OIT depletion has yet to be described.

A drop in squeeze-out Std-OIT with reducing speed was also observed for the two other WW130 welding temperature cases examined, 352 °C and 460 °C (Fig. 8). Unlike the 400 °C temperature series, these two series did not display as clear a Std-OIT depletion threshold for the welding speeds examined. Instead, the 352 °C series exhibited the

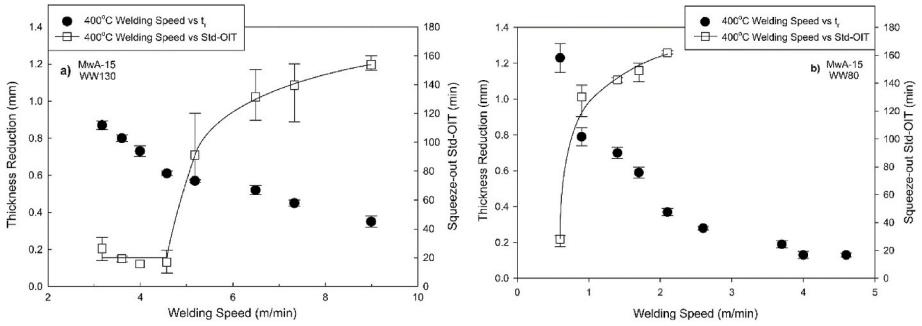

Fig. 6. Squeeze-out Std-OIT depletion with respect to seam thickness reduction for WW130 and WW80 seam series. Seam series were created for sheet temperatures of 21 °C using the manufacturer recommended seaming temperature of 400 °C and seaming force. In both series, Std-OIT dropped gradually until a critical welding speed is reached, at which point they precipitously fall to a residual value of approximately 20 min.

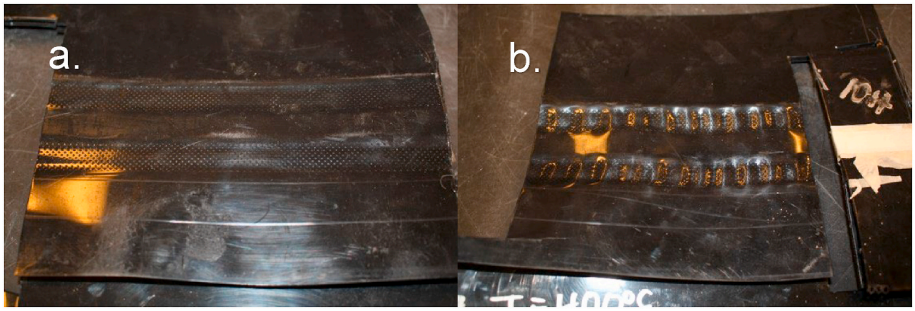

Fig. 7. Seam rippling, a qualitative sign of overheating, occurs when heat applied to the seam reaches a level high enough to melt a significant portion of the sheets thickness, in turn permanently deforming the weld as the nip rollers apply pressure. This qualitative sign of overheated was noted to occur shortly after Std-OIT values dropped precipitously to a residual value for the WW130 and WW80 wedge welders, suggesting this may serve as a qualitative indication of squeeze-out Std-OIT loss. 7a is a typical smooth weld zone track that indicates a weld that is not over heated, 7b shows weld zone rippling that occurred at approximately 0.6 mm thickness reduction for the WW130 wedge welder.

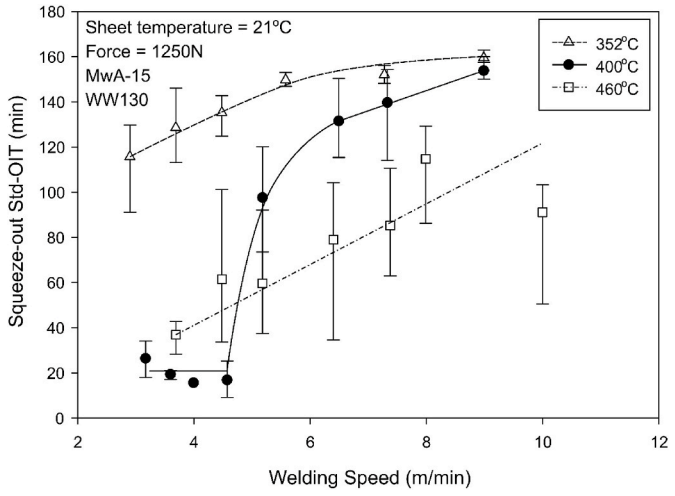

Fig. 8. Variation in MwA-15 squeeze-out Std-OIT for three seam series created using WW130 and with wedge temperatures of 352 °C, 400 °C and 460 °C. Seaming pressure and surface temperature at the time of welding for all three series was set to 1250N and 21 °C, respectively.

near linear start of Std-OIT loss with reducing speed at approximately 6–7 m/min. This reduction continued until a burn out was achieved at approximately 2.9 m/min, at which point the range in recorded Std-OIT values increased to a series maximum, suggesting, if a burn out failure was not achieved, that any further reduction in welding speed would start to significantly reduce squeeze-out Std-OIT (like that of the 400 °C series). This means that the entire range of speeds examined for the 352 °C series did not result in as significant a drop in Std-OIT as the other two welding temperatures, and instead resulted in a burn out failure before near full antioxidant depletion could occur. Conversely, the 460 °C series, which started at 10 m/min, exhibited more substantial antioxidant depletion from the start, with an average Std-OIT value of 91 min (max and min of 103 min and 62 min, respectively). After this point, there was a gradual reduction in average squeeze-out Std-OIT with increasing welding speed down to a value close to that of the 400 °C series at 3.7 m/min. It is expected that further increases in welding speed would eventually result in a leveled off Std-OIT closer to the sheet value, similar to that observed for the 352 °C and 400 °C series. Even at comparatively fast speeds some antioxidant depletion was detected for the 460 °C series, suggesting it's possible that this welding temperature, partially due to the increased wedge size of this machine, could result in at least partial Std-OIT loss for this material when thickness reduction is within the DVS 2225-3 0.2–0.6 mm range. This temperature was 60 °C above the manufacturer's recommended welding temperature of 400 °C for a 1.5 mm HDPE GMB. Variation in recorded Std-OIT values for the 460 °C series was higher than that of the 400 °C and 352 °C series, despite Std-OIT values having dropped to near 20 min residual levels at lower speeds. The increased variability is hypothesized to be the result of inconsistent mixing of the polymer melt and additive heterogeneity within the squeeze-out. Higher wedge seaming temperatures may have the potential to melt material adjacent to, but not in contact with, the hot wedge during seaming, resulting in antioxidant heterogeneity in the squeeze-out as molten polymer from both the wedge/sheet interface and material adjacent to this interface are forced together forming squeeze-out. This increased variability with increasing applied heat is consistent with the 400 °C and 352 °C series, where squeeze-out Std-OIT variability generally increases with decreasing speed until a threshold is achieved. Once the welding speed is low enough, the majority of the melt has been heated enough to exhibit near full antioxidant depletion, effectively reducing the range of recorded values.

Squeeze-out Std-OIT was found to decrease with decreasing weld speed, thickness reduction and increased seaming wedge temperature. Welding speed reduction resulted in a gradual decreasing in Std-OIT until a critical speed was reached, at which point Std-OIT values dropped precipitously and seam rippling could be observed in some seams. Using WW130 at a 460 °C welding temperature resulted in antioxidant depletion in seams with acceptable thickness reductions based on DVS 2225-3 (0.2–0.6 mm). Suggesting, this seaming temperature should be avoided in order to mitigate antioxidant loss within the seams squeeze-out, particularly when using a larger length wedge welder and seaming at warm temperatures. Seam rippling should also be avoided as seams with weld track rippling were found to exhibit a higher degree of antioxidant loss than those without.

3.4. Welding pressure

The effect of welding pressure on squeeze-out antioxidant depletion was examined for three different nip roller force settings. One of the two wedge welders used in this study (WW130) provided a digital display with continuous force measurements made available through the built-in load cell atop the machines nip rollers. This provided the basis for a quantitative examination into the effect of welding force, however, as nip roller geometry may vary between welding machines, the actual applied pressure acting on the geomembrane being seamed may vary between machines for a given applied nip roller force. Furthermore, recorded force measurements were taken prior to the addition of heat, and as such, represent the force applied onto to the geomembrane overlap during equipment setup. This is an important distinction as changes to welding temperature and speed alter the degree of melting which occurs during seaming, resulting in changes in squeeze-out amount and a seaming force which may differ from the initial setup force. In an effort to provide testing repeatability, force measurements were taken during machine setup and resulting thickness reduction and squeeze-out std-OIT results are assumed to incorporate the synergistic effects other welding parameters may have on the seaming force while the machine is in operation.

Seaming force was set 170N above (1420N), at 1250N, and 180N below (1070N) the manufacturer's recommended value. Seaming temperature was set to 400 °C to remain consistent with manufacturer guidelines. Fig. 9a shows the relationship between thickness reduction

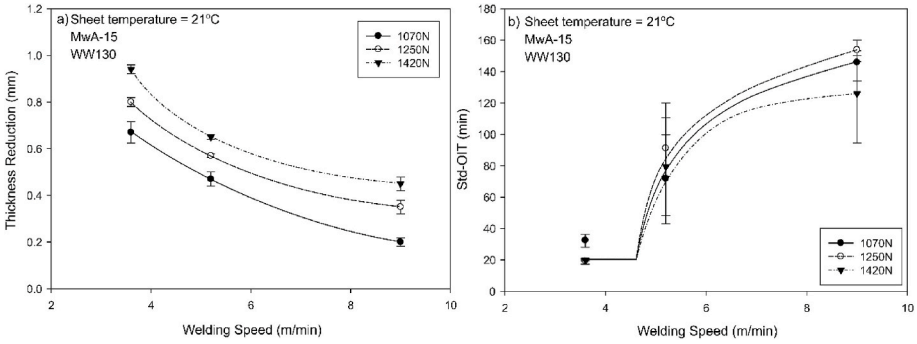

Fig. 9. Variation in MwA-15 thickness reduction (9a) and squeeze-out Std-OIT loss (9b) for three seam series created using the WW130 wedge welder. Seaming temperature and sheet temperature at the time of welding were set to 400 °C and 21 °C, respectively. Despite the observed variation in seam thickness reduction, Std-OIT loss was reasonably consistent between welding speeds, particularly when welding speeds were ≤5.2 m/min. This suggests that seaming pressure has a limited effect on the heat applied to the seam and that sheet temperature at the time of welding, welding wedge temperature, and welding speed greater influence squeeze-out Std-OIT loss.

and the three welding pressure cases examined. An increase in thickness reduction with increasing seaming pressure was observed for each of the welding speeds examined, with the highest seaming force producing the greatest thickness reduction. The difference in thickness reduction between the each of the seaming forces examined at any of the welding speeds was approximately 0.1 mm. However, it is expected with further increases in welding speed all three series would approach 0 mm thickness reduction. Despite this, the 1420N and 1070N series displayed a nonlinear seam thickness reduction vs welding speed relationship, like that of the other 1250N series (Fig. 5). Because only 3 data points were collected, exponential curves were not fitted to these data.

Fig. 9b shows the squeeze-out Std-OIT for each of the seams created using different seaming forces. For each of the welding speeds examined, changes in seaming force resulted in a similar squeeze-out Std-OIT and a drop to a potential residual value of approximately 20 min at 3.6 m/min. The 1420N series at 9 m/min welding speed exhibited a slightly lower Std-OIT than the other seaming force cases. This was attributed to higher seaming pressure being more effective at forcing out potential antioxidant depleted melt from the weld zone. However, as the range of values were high and Std-OIT values between the three seaming forces at speeds ≤5 0.2 m/min were effectively equal, this difference was not attributed to increased heat addition to the polymer melt. The Std-OIT transition speed of 5.2 m/min was also consistent for the 1420N and 1070N series and exhibited high variation among sample values, consistent with what was previously observed for the WW130 1250N series (Fig. 6a). It appeared that, although the amount of squeeze-out increased with increasing seaming pressure, the amount of heat added to the seam remained reasonably consistent for each of the cases, particularly at speeds ≤5.2 m/min. This is likely because the nip rollers force partially molten sheets together after the hot wedge has passed, resulting in welding pressure having a limited effect on the amount of heat added to the geomembrane during seaming. Despite this, an increased amount of squeeze-out and thickness reduction may have its own potential issues regarding stress cracking and changes in seam geometry resulting in strain concentration (Kavazanjian et al., 2017; Peggs 2019; Francey and Rowe, 2021).

For a given welding speed and temperature, seaming force was found to have a limited effect on squeeze-out antioxidant loss. This is due to changes in seaming force having a minimal effect on the amount of heat added to the GMB during seaming. Changes in seaming force were found to alter the amount of squeeze-out produced and subsequent thickness reduction in HDPE seams, suggesting that any guidelines in place limiting the extent of thickness reduction consider a range of acceptable seaming forces. This is significant in that any correlation between thickness reduction and other physical/chemical properties of a seam (e.g., antioxidant loss) must include seams that extend a range of seaming forces. Moreover, changes to seaming force that allow a previously failed qualification seam to pass seam peel/shear tensile criteria may be conducted with little concern regarding the extent of antioxidant loss in the squeeze-out. However, the effect of increase squeeze-out production on seam SCR should still be considered when change seaming force in field.

4. Discussion

4.1. Thickness reduction and Std-OIT relationship

Squeeze-out Std-OIT has been examined for a total of 59 seams welded at 3 different seaming temperatures and pressures for 3 GMBs and 3 sheet temperatures at the time of welding. Thickness reduction was found to provide an indication of squeeze-out Std-OIT depletion for the welds examined, where on average greater thickness reduction welds exhibited greater Std-OIT loss. Thickness reduction has been plotted against squeeze-out Std-OIT loss to allow identification of thickness reduction thresholds, or ranges, at which Std-OIT loss was observed (Figs. 10–12).

4.1.1. Effect of wedge temperature

Greater wedge temperatures increased heat transfer to the polymer, increasing the likelihood of antioxidant depletion. Fig. 10 illustrates the relationship between squeeze-out Std-OIT and thickness reduction for three MwA-15 seam series produced using the WW130 wedge welder at wedge temperature settings of 352 °C, 400 °C, and 460 °C, a nip roller force of 1250N, welding speeds of 2.9–10 m/min, and a sheet temperature of 21 °C.

Starting at about Std-OIT ~160 min, there was negligible decrease in OIT at 0.2 mm thickness reduction for the lowest wedge temperature

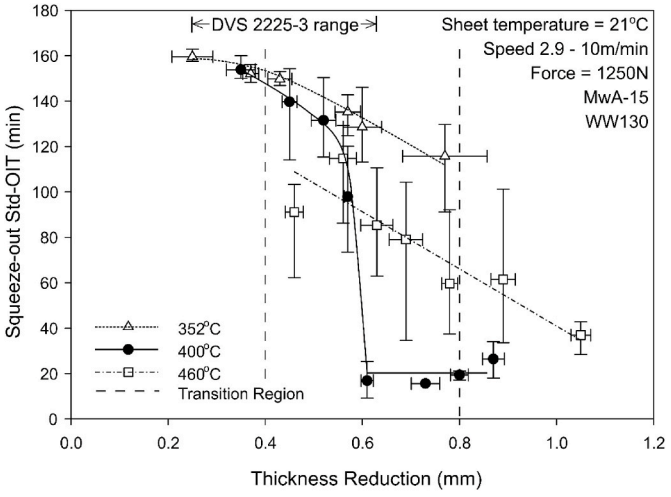

Fig. 10. MwA-15 squeeze-out Std-OIT depletion plotted against seam thickness reduction for the three wedge temperature series welded using the WW130 wedge welder. Thickness reduction transition region was set based on the observed drop in Std-OIT values for seams exhibiting thickness reductions <0.4 mm, and seams displaying near full Std-OIT depletion when thickness reduction is > 0.8 mm.

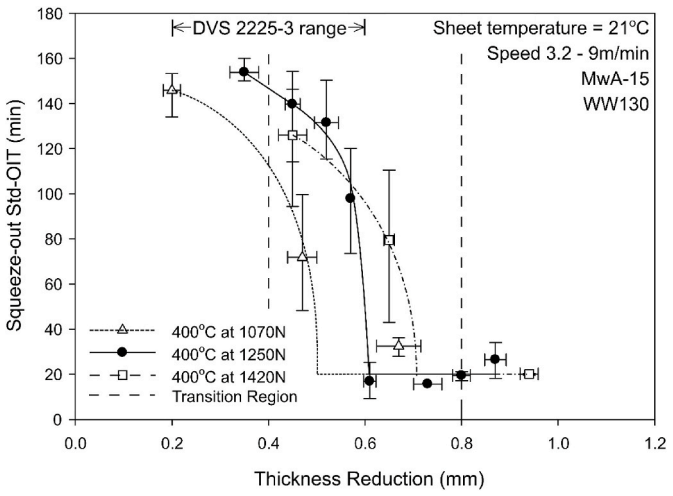

Fig. 11. MwA-15 Squeeze-out Std-OIT depletion plotted against seam thickness reduction for the three seaming force series welded using the WW130 wedge welder. Thickness reduction transition region was set based on the observed drop in Std-OIT values for seams exhibiting thickness reductions <0.4 mm, and seams displaying near full Std-OIT depletion when thickness reduction is > 0.8 mm.

(352 °C). This was followed by a decrease in Std-OIT at a thickness reduction of 0.3–0.4 mm that continued until a Std-OIT ~120 min at a welding speed of 2.9 m/min, just before burnout failure. No 352 °C seams produced by the WW130 welder at the pre-burnout welding speeds examined (2.9–9 m/min) approached complete Std-OIT depletion regardless of thickness reduction.

At the welding speeds examined, the 400 °C series exhibited a similar onset to Std-OIT reduction at ~0.3–0.4 mm thickness reduction, although Std-OIT values dropped precipitously down to a residual once thickness reduction reached ~0.6 mm at a speed of ~5 m/min. This suggests that, for this welding temperature and wedge welder, thickness reductions >0.5 mm are potentially problematic and reductions ≥0.6 mm should be avoided.

The 460 °C series exhibited increased Std-OIT variability and relatively low Std-OIT values when thickness reductions were ≥0.45 mm (a value within the allowable DVS 2225-3 range) and hence welding speeds <10 m/min. Moreover, near full Std-OIT reduction was achieved once thickness reductions exceeded ~0.8 mm–0.9 mm or welding speed ≤5 m/min.

For the material and range of welding temperatures examined (352 °C–460 °C), an initial drop in squeeze-out Std-OIT was detected when seam thickness reductions surpassed 0.4 mm and low to very low Std-OIT values when thickness reductions were ≥0.6 mm. The welding temperature 460 °C exhibited an increased potential for Std-OIT loss when thickness reductions fell within the DVS 2225-3 range. Thus, 460 °C was consider too high a welding temperature based on the potential for squeeze-out Std-OIT loss when welding at sheet temperatures >0 °C. There may be benefit to this higher welding temperature at low sheet temperatures.

4.1.2. *Effect of welding force*

Using the observed drop in Std-OIT for seams formed by the WW130 welder at 400 °C wedge temperature, 1250N seaming force, welding speeds from 3.2 to 9 m/min, and a sheet temperature of 21 °C (Fig. 10), a similar Std-OIT/thickness reduction interpretive curve was used to describe Std-OIT reduction for both the 1070N and 1420N series (Fig. 11). Changes in seaming force were found to create a shift in the degree of Std-OIT loss for a given thickness reduction. This relationship was most apparent within the 0.4 mm–0.8 mm thickness reduction transition region at corresponding thickness reductions of approximately 0.45 mm, 0.55 mm, and 0.65 mm, for the 1070N, 1250N, and 1420N series, respectively. For the material and welding equipment examined, an approximately 14% deviation from the manufacturer recommended seaming force resulted in an ~0.1 mm shift in the thickness reduction necessary to achieve a specific degree of Std-OIT reduction. Thus, the thickness reductions resulting in residual Std-OIT (~20 min) were approximately 0.5 mm, 0.6 mm, and 0.7 mm for the 1070N, 1250N, and 1420N series, respectively. Thus, a change in the seaming force from the manufacturer specified value may produce seams with lower squeeze-out Std-OIT values when thickness reductions are within the DVS 2225-3 range, with a force reduction having greater

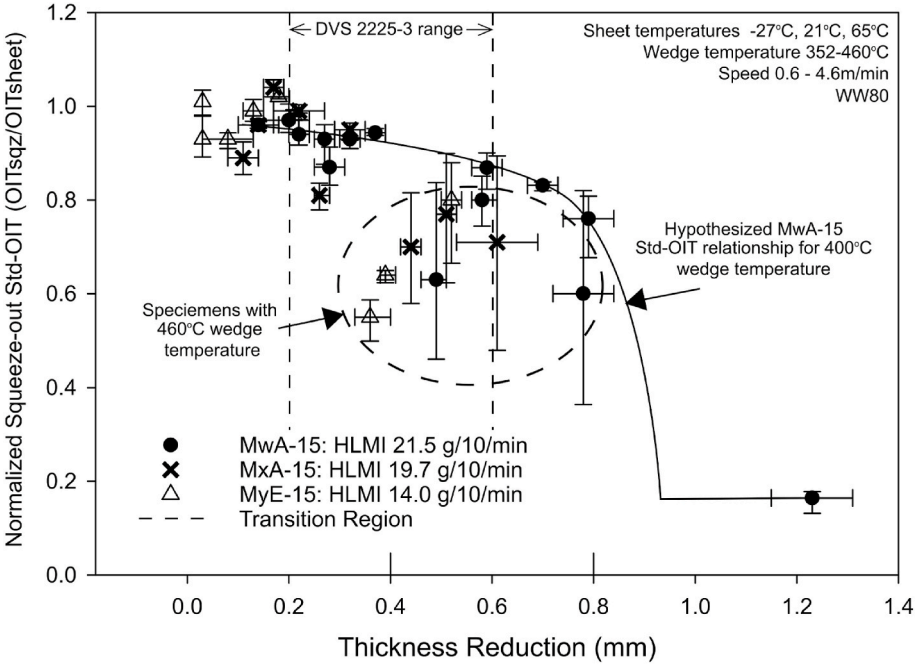

Fig. 12. Squeeze-out Std-OIT depletion plotted against seam thickness reduction for the three geomembranes welded using the WW80 wedge welder. DVS 2225-3 thickness reduction range was plotted to illustrate the observed drop in squeeze-out Std-OIT for seams created using a 400 °C wedge temperature.

effect on squeeze-out OIT than an increased force within this range. Furthermore, increasing thickness reduction increased the squeeze-out from the welded zone, with greater force increasing thickness reduction, subsequently producing greater squeeze-out.

Despite this, seams examined within this seaming force range exhibited modest (i.e., less than 30% for a force reduction less than 14%) Std-OIT depletion when thickness reductions were ~0.4 mm. Thus, attempting to achieve a 0.4 mm thickness reduction is likely to provide redundancy even when accounting for changes in weld seaming force. In terms of antioxidant loss, welding temperature and speed appear to be the governing controls on Std-OIT reduction in the squeeze-out. However, an increase in seaming force may also have implications in seam SCR, as increased squeeze-out production may increase the likelihood of squeeze-out adherence and the creation of deleterious geometries leading to lower seam SCR (Francey and Rowe, 2021). The results presented herein combined with the findings of Francey and Rowe (2021) suggests that one should maintain the manufacturer specified seaming force whenever possible. If this is not possible and the force is reduced, the DVS 2225-3 maximum thickness reduction criteria should be reduced.

4.1.3. Wedge size and material effect

To assess the effect of wedge size and differences between materials on the thickness reduction squeeze-out Std-OIT relationship three series of welds were produced using the smaller WW80 welder. Each of these series include welds produced at three geomembranes sheet temperatures ranging from −27 °C to 65 °C and wedge temperatures ranging from 352 °C to 460 °C and welding speeds from 1.8 m/min - 3.0 m/min (Table 3). In addition, one extra series of MwA-15 welds, produced using WW80, a 400 °C welding temperature, a sheet temperature of 21 °C, and speeds ranging from 0.6 m/min – 4.6 m/min were included in this analysis (from Fig. 6b).

Fig. 12 illustrates the thickness reduction squeeze-out Std-OIT relationship for the three materials examined. Partial squeeze-out Std-OIT loss was observed in all three materials, with MwA-15, the flat die geomembrane, exhibiting one weld with almost full Std-OIT depletion. Much like the previous relationships observed in Figs. 10 and 11, the loss in squeeze-out Std-OIT was relatively low for thickness reductions <0.4 mm for the two geomembranes with a high HLMI (MwA-15 and MxA-15), but MyE-15 (with HLMI = 14) had lost about 40% of its initial Std-OIT for thickness reductions just less than 0.4 mm. For the two geomembranes with a high HLMI the drop in Std-OIT was initiated once thickness reduction exceeded >0.4 mm. None of the welds within the 0.4 mm–0.8 mm transition region experienced a Std-OIT reduction approaching the residual value. Instead, in all cases the normalized Std-OIT values ranged between ~0.55–1.0. This suggests that smaller wedge welders may produce welds with relatively less squeeze-out Std-OIT loss, for a given thickness reduction, than the large ones. This is most apparent when comparing the MwA-15 WW80 400 °C Std-OIT relationship (Fig. 12) with that of the MwA-15 WW130 400 °C relationship (Fig. 10), where ~20 min values are reached at >0.8 mm and ~0.6 mm thickness reduction, respectively. Less heat addition resulting from a decreased sheet/wedge contact time for a given welding speed was thought to have contributed to the relatively higher Std-OIT values for a given thickness reduction. Alternatively, the seaming force for the smaller WW80 wedge welder, which was qualitatively set by the operator as per manufacturer guidelines, may have induced greater seaming stress than WW130, effectively increasing the degree of thickness reduction necessary to achieve a given degree Std-OIT loss (similar to that shown in Fig. 11). However, considering WW80 was calibrated following manufacturer specifications, it may be reasonable to assume that for a given thickness reduction smaller wedge welders produce welds with less squeeze-out Std-OIT loss.

MyE-15, a blown film GMB with a lower HLMI value than MwA-15, exhibited the greatest Std-OIT loss for a given thickness reduction of seams created using a 460 °C wedge temperature (Fig. 12). This is attributed to the difference in HLMI effectively limiting the flow of molten polymer from the weld zone to squeeze-out. The relationship between HLMI for the materials and their corresponding 9 welding parameter combinations (Table 3) can be seen in Fig. 13, where on average the greater the HLMI the greater the degree of thickness reduction a weld may experience for a given set of welding parameters. MyE-15 exhibited upwards of ~45% squeeze-out Std-OIT loss at approximately 0.35 mm thickness reduction while MwA-15 required upwards of ~0.5–0.8 mm thickness reduction to achieve a similar degree of Std-OIT loss (for 460 °C seams). Thus, it is inferred that the thickness reduction necessary to reach residual Std-OIT levels experienced by MwA-15 at 400 °C may be lower for MyE-15 and MxA-15. The decrease in Std-OIT was limited to <30% loss in seams with ≤0.8 mm thickness reduction for the MwA-15 400 °C WW80 wedge temperature series (Fig. 12). Thus, this value represents a conservative thickness reduction threshold for maintaining a relatively high squeeze-out Std-OIT with the WW80 welder at a 400 °C wedge temperature for geomembranes with a HLMI ≈21.5g/10 min. Assuming the slope of the thickness reduction/HLMI relationship (Fig. 13) remains constant for different thickness reduction levels, this equation was used to estimate a conservative MyE-15 thickness reduction limit (for a 400 °C wedge temperature) by applying a vertical shift to the equation (i.e., slope remains 0.0192) such that it passed through the MwA-15 conservative

Table 3
Welding parameter combinations used for the three materials. Each material was welded at three different sheet temperatures using 3 different wedge welder temperature and speed combinations for a total of 27 unique welds. Specific combinations are referred to using number and letter combinations (e.g MwA-15 1a was created using the MwA-15 product, a sheet temperature of 60 °C, a wedge temperature of 460 °C, and a welding speed of 1.8 m/min, etc).

Materials and Parameters Examined	Sheet Temperature at Time of Welding	
	65 ± 5 °C (1), 21 ± 1 °C (2), −27 ± 2 °C (3)	
	Welding Wedge Temperature (°C)	Welding Speed (m/min)
MwA-15	460 (a)	1.8 (a)
MxA-15	400 (b)	3.0 (b)
MyE-15	352 (c)	2.6 (c)

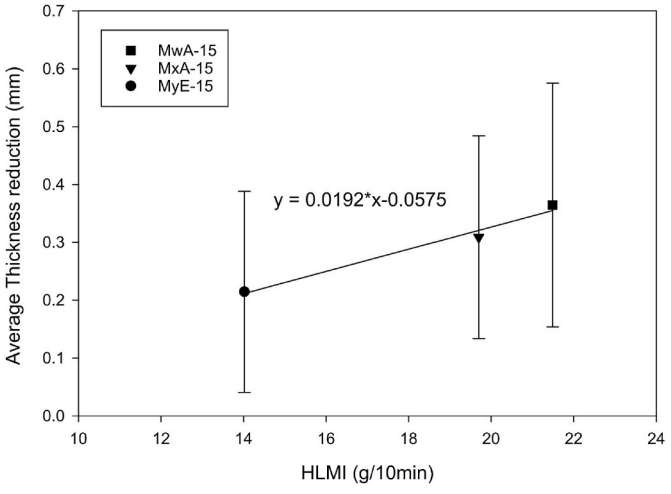

Fig. 13. Variation in thickness reduction with respect to high-load melt index (HLMI) between the three materials examined. Seam series utilized welding parameters outlined in Table 3, where the same set of 9 welding speed, wedge temperature, and sheet temperature at the time of welding combinations were used for each material. On average higher HLMI materials displayed greater thickness reduction, which may influence the aforementioned thickness reduction vs Std-OIT relationship. Error bars represent one standard deviation of thickness reduction measurements.

thickness reduction threshold (x = 21.5g/10min, y = 0.8 mm). The 400 °C wedge temperature MyE-15 conservative thickness reduction threshold was estimated to be ~0.66 mm, a value higher than the DVS 2225-3 limit. Thus, it was hypothesized that a wedge temperature of 400 °C, for WW80, would produce suitable seams (i.e., those without substantial squeeze-out Std-OIT loss) for seams within the DVS 2225-3 thickness reduction range.

The evidence suggests that the geomembrane's HLMI influenced the degree of thickness reduction a seam will experience, where higher HLMI GMBs experience greater thickness reduction than lower HLMI GMBs for the same welding parameters. This suggests that welding practices incorporating lower HLMI GMBs (e.g., 14 g/10min) should place increased emphasis on targeting the lower end of the DVS 2225-3 thickness reduction range (i.e., 0.2 mm–0.4 mm). No WW80 seams exhibited near zero Std-OIT values when thickness reductions fell within the DVS 2225-3 thickness reduction range. However, all WW80 seams utilizing a 460 °C wedge temperature, and in particular the lower HLMI MyE-15(Fig. 12), showed an increased potential for Std-OIT loss when thickness reductions fell between ~0.4 mm and 0.6 mm (similar to that of Fig. 10). This, in conjunction with the WW130 460 °C Std-OIT reduction in Fig. 10, implies that a 460 °C weld temperature should be avoided for both welding machines for seams created with a sheet temperature >0 °C, and that one should attempt to attain 0.2 mm–0.4 mm thickness reduction while not exceeding 0.6 mm.

5. Practical implications and Application's

The data presented and discussed above implies that dual track fusion welding of HDPE GMBs has the potential to deplete antioxidants within the seams squeeze-out. Further research is needed to examine whether this may ultimately lead to faster degradation of the polymer and faster loss in stress crack resistance at a critical location. However, previous research has shown the significance of squeeze-out geometry and adherence on seam SCR (Francey and Rowe, 2022), as well as the potential for faster than sheet Std-OIT depletion in a seams HAZ (Rowe and Shoaib 2018). Together these previous findings highlight the importance of both monitoring seam squeeze-out and limiting the degree of antioxidant loss within seams.

Wedge temperatures of 460 °C resulted in greater Std-OIT variation and, in some cases, a high degree squeeze-out Std-OIT loss for seams within the DVS 2225-3 thickness reduction range of 0.2–0.6 mm for a 1.5 mm geomembrane (Figs. 10 and 12). Although it may be possible to produce seams with relatively little squeeze-out Std-OIT loss at a 460 °C wedge temperature (e.g., utilizing a higher welding speed than that examined), it would be prudent to avoid this temperature in the fusion welding of 1.5 mm GMBs when sheet temperatures are greater than 0 °C. While seaming at sub-zero sheet temperatures, the additional heat added by this higher wedge temperature may help produce stronger welds, particularly for materials with a higher HLMI (>14g/10min). HLMI has shown to shift the degree of Std-OIT loss for a given thickness reduction a seam may experience. Fusion welding of material with a HLMI ~14g/10min at 460 °C exhibited a notable drop in squeeze-out Std-OIT when the thickness reduction was as low as ~0.3 mm–0.4 mm (Fig. 12). Thus, when welding geomembranes with a HLMI ≤14g/10min, one should place increased emphasis on maintaining thickness reduction from 0.2mm to 0.4 mm and avoid wedge temperatures >430 °C when welding at sheet temperatures >0 °C.

Likewise, lower nip roller forces resulted in lower squeeze-out Std-OIT values for a given thickness reduction. The potential for seaming force to alter the suitability of the DVS 2225-3 range (based on squeeze-out Std-OIT retention) leads to the conclusion that operators should, whenever possible, employ the manufacturer specified seaming force (or means of qualitatively setting it). If seaming force must be modified (e.g., ±14% the manufacture recommended value) care should be taken to estimate an appropriate shift in the acceptable thickness reduction range (Fig. 11).

Due to increased wedge/sheet contact time for WW130, larger wedge welders can produce seams within a desired thickness reduction range faster than small ones (Fig. 6). To meet a target thickness reduction (e.g., reaching 0.2 mm–0.4 mm), the welding speed can be adjusted on trial seams prior to welding of panel overlaps. This should be done considering the non-linear relationship between welding speed and thickness reduction, where a unit change in welding speed results in a greater unit change in thickness reduction when welding speeds are decreased then when increased.

For the range of materials, equipment, and welding parameters examined, HDPE seam thickness reduction has shown to be an important indicator in several ways.

(a) Squeeze-out antioxidant depletion was found to drop significantly for thickness reductions greater than ~0.4 mm–0.6 mm (Figs. 10–12) and seams with more than 0.8 mm thickness reduction generally displayed near full antioxidant depletion within the squeeze-out (Figs. 10–12).
(b) Seam rippling occurred for thickness reductions in the 0.6 mm–0.8 mm range coinciding with a large decrease in squeeze-out Std-OIT (Figs. 6 and 7).
(c) Seam burn out failures occurred when thickness reductions were ~0.8 mm or greater (Table 2).
(d) The DVS 2225-3 limits thickness reduction for a 1.5 mm thick geomembrane to between 0.2 mm and 0.6 mm.

The latter three observations provide support for the DVS recommendations but combined the four observations lead towards a conclusion that engineers monitoring seam thickness reduction should generally maintain 0.2 mm–0.4 mm thickness reduction and avoid exceeding 0.6 mm thickness reduction when welding a 1.5 mm HDPE GMB. During geomembrane installation quality assurance, weld thickness reduction criteria can be implemented alongside GRI-GM19 strength/ductility criteria (ASTM D 6392) to help mitigate potential long-term damage to the geomembrane during installation.

6. Conclusions

This study examined the squeeze-out antioxidant depletion of HDPE dual track fusion welds created from three different materials (denoted MxA-15, MwA-15, and MyE-15) under a range of welding parameter combinations. Seams were welded by an experienced geomembrane installer using two different wedge welders with heating element lengths of ~130 mm and ~80 mm. This study has shown that the movement of molten polymer from the weld zone to adjacent heat affect zones in the form of squeeze-out contributes to heat transfer away from the hot wedge/sheet interface towards the extremities, or HAZs, of the welds examined. Squeeze-out has been found to be partially to almost fully depleted in Std-OIT as a result of welding practices, serving as both a metric for the heat applied during welding, but also having the potential to influence a seams SCR in the event squeeze-out adherence occurs onto the HAZ (Peggs, 2019; Francey and Rowe, 2022). The results of this study have also shown that, for the GMBs, welding equipment, and conditions examined:

1. Heat transfer to a seams HAZ largely comes from the movement of molten polymer in the form of squeeze-out. Thus, monitoring squeeze-out can provide insight into the heat added to a seam during welding.
2. For a given thickness reduction and quality of weld the larger (~130 mm) heating wedge WW130 could create welds at much greater speed than the smaller (~80 mm) WW80 machine.
3. On average, and for a given set of welding parameters, higher HLMI geomembranes experienced a greater degree of thickness reduction than lower HLMI geomembranes. Thus, seaming of lower HLMI GMBs (e.g., HLMI ≤14.0 g/10min) should generally incorporate

lower heat applied welding parameters and put increased emphasis on targeting thickness reductions within the lower half of the DVS 2225-3 range (i.e., 0.2 mm–0.4 mm).

4. Seaming force alters both the degree of thickness reduction and amount of squeeze-out produced while having a limited effect on altering the amount of heat added to a seam. Thus, for the purpose of adhering to the DVS 2225-3 range, seaming force should be set to the manufacturer specified value whenever possible and when not, consideration must be given to the corresponding lowering of the upper acceptable thickness reduction limit (Fig. 11).
5. For the materials, equipment, and welding parameters examined, adherence to the DVS 2225-3 thickness reduction range, served as a useful criterion for producing seams with the intent of limiting squeeze-out Std-OIT loss.

Acknowledgments

The research was funded by Strategic Grant STPGP521237 – 18 from the Natural Sciences and Engineering Research Council of Canada (NSERC). In-kind support was provided by Titan Environmental and Leister Technologies AG. Funding for the development of the research infrastructure was provided by the Canada Foundation for Innovation, the Ontario Innovation Trust, the Ontario Research Fund Award, and Queen's University under project 36663. The support of all those listed above is much appreciated; however, the opinions expressed in the paper are solely those of the authors.

Notations

Std-OIT	standard oxidative induction time (s)
HP-OIT	high pressure oxidative induction time (s)

Abbreviations

HDPE	high density polyethylene
GMB	geomembrane
HAZ	heat-affected zone of the seam
CQA	construction quality assurance
WW130	larger wedge welder used with an ~130 mm wedge length
WW80	smaller wedge welder used with an ~80 mm wedge length

References

Abdelaal, F.B., Rowe, R.K., Islam, M.Z., 2014. Effect of leachate composition on the long-term performance of a HDPE geomembrane. Geotext. Geomembranes 42 (4), 348–362.

Abdelaal, F.B., Rowe, R.K., 2015. Durability of three HDPE geomembranes immersed in different fluids at 85 C. J. Geotech. Geoenviron. Eng. 141 (2), 04014106.

Abdelaal, F., Rowe, R., 2019. Degradation of an HDPE geomembrane without HALS in chlorinated water. Geosynth. Int. 26 (4), 354–370.

Abdelaal, F., Morsy, M., Rowe, R.K., 2019. Long-term performance of a HDPE geomembrane stabilized with HALS in chlorinated water. Geotext. Geomembranes 47 (6), 815–830.

ASTM D1238, 2013. Standard Test Method for Melt Flow Rates of Thermoplastics by Extrusion Plastometer. American Society for Testing and Materials D1238, West Conshohocken, PA, USA.

ASTM D3895, 2019. Standard Test Method for Oxidative-Induction Time of Polyolefins by Differential Scanning Calorimetry. American Society for Testing and Materials D3895, West Conshohocken, PA, USA.

ASTM D5199, 2019. Standard Test Method for Measuring the Nominal Thickness of Geosynthetics. American Society for Testing and Materials D5199, West Conshohocken, PA, USA.

ASTM D5397, 2007. Standard Test Method for Evaluation of Stress Crack Resistance of Polyolefin Geomembranes Using Notched Constant Tensile Load Test. American Society for Testing and Materials D5397, West Conshohocken, PA, USA.

ASTM D5885, 2006. Standard Test Method for Oxidative Induction Time of Polyolefin Geosynthetics by High-Pressure Differential Scanning Calorimetry. American Society for Testing and Materials D5885, West Conshohocken, PA, USA.

ASTM D6392, 2012. Standard Test Method for Determining the Integrity of Nonreinforced Geomembrane Seams Produced Using Thermo-Fusion Methods. American Society for Testing and Materials D6392, West Conshohocken, PA.

ASTM D6693, 2004. Standard Test Method for Determining Tensile Properties of Nonreinforced Polyethylene and Nonreinforced Flexible Polypropylene Geomembranes. American Society for Testing and Materials D6693, West Conshohocken, PA, USA.

Di Battista, V., Rowe, R.K., 2020. TCE and PCE diffusion through five geomembranes including two coextruded with an EVOH layer. Geotext. Geomembranes 48 (5), 655–666.

DVS 2225-3. "Welding of Linging Membranes Made of polyethylene(PE) for the Protection of Groundwater."German Welding Society, Düsseldorf, Germany.

Ewais, A.M.R., Rowe, R.K., Scheirs, J., 2014. Degradation behaviour of HDPE geomembranes with high and low initial high-pressure oxidative induction time. Geotext. Geomembranes 42 (2), 111–126.

Francey, W, Rowe, R K, 2022. Stress crack resistance of unaged high-density polyethylene geomembrane fusion seams. Geosynthetics International, 10.1680/jgein.21.00027a.

Giroud, J., Tisseau, B., Soderman, K., Beech, J., 1995. Analysis of strain concentration next to geomembrane seams. Geosynth. Int. 2 (6), 1049–1097.

GRI-GM19. "Seam Strength and Related Properties of Thermally Bonded Polyolefin Geomembranes."Geosynthetic Research Institute, PA, USA.

GRI-GM13. "Standard Specification for Test Methods, Test Properties, and Testing Frequency for High Density Polyethylene (HDPE) Smooth and Textured Geomembranes."Geosynthetic Research Institute, PA, USA.

Halse, Y., Koerner, R., Lord, A., 1990. Stress cracking morphology of polyethylene (PE) geomembrane seams. In: Geosynthetics: Microstructure and Performance, ASTM International.

Hsuan, Y., Koerner, R., 1998. Antioxidant depletion lifetime in high density polyethylene geomembranes. J. Geotech. Geoenviron. Eng. 124 (6), 532–541.

Hsuan, Y.G., Schroeder, H.F., Rowe, R.K., Müller, W., Greenwood, J., Cazzuffi, D., Koerner, R.M., 2008. Long-term Performance and Lifetime Prediction of Geosynthetics". 4th European Conference on Geosynthetics. Edinburgh, September, Keynote paper.

Hsuan, Y.G., 2000. Data base of field incidents used to establish HDPE geomembrane stress crack resistance specifications. Geotext. Geomembranes 18 (1), 1–22.

Kavazanjian, E., Andresen, J., Gutierrez, A., 2017. Experimental evaluation of HDPE geomembrane seam strain concentrations. Geosynth. Int. 24 (4), 333–342.

Li, W., Xu, Y., Huang, Q., Liu, Y., Liu, J., 2021. Antioxidant depletion patterns of high-density polyethylene geomembranes in landfills under different exposure conditions. Waste Manag. 121, 365–372.

Müller, W.W., 2007. HDPE Geomembranes in Geotechnics. Springer.

McWatters, R., Rowe, R., Di Battista, V., Sfiligoj, B., Wilkins, D., Spedding, T., 2020. Exhumation and performance of an Antarctic composite barrier system after 4 years exposure. Can. Geotech. J. 57 (8), 1130–1152.

Morsy, M., Rowe, R.K., 2020. Effect of texturing on the longevity of high-density polyethylene (HDPE) geomembranes in municipal solid waste landfills. Can. Geotech. J. 57 (1), 61–72.

Morsy, M.S., Rowe, R.K., Abdelaal, F.B., 2021. Longevity of 12 geomembranes in chlorinated water. Can. Geotech. J. 58 (4), 479–495.

Peggs, I.D., Carlson, D.S., 1990. Brittle fracture in polyethylene geomembranes. In: Geosynthetics: Microstructure and Performance, ASTM International.

Peggs, I.D., Carlson, D.S., 1990b. The effects of seaming on the durability of adjacent polyethylene geomembranes. In: Geosynthetic Testing for Waste Containment Applications, ASTM International.

Peggs, I.D., Carlson, D.S., Peggs, S.J., 1990. Understanding and preventing 'shattering' failures of polyethylene geomembranes. In: Proc., Proceedings of the Fourth International Conference on Geotextiles, Geomembranes and Related Products, AA Balkema, Rotterdam, Netherlands, pp. 549–553.

Peggs, I., Gassner, F., Scheirs, J., Tan, D., Arango, A., Burkard, B., 2014. Is there a resurgence of stress cracking in HDPE geomembranes. In: Proc., Proceedings of the 10th International Conference on Geosynthetics, Berlin.

Peggs, I.D., 2019. Impact of Microstructure on HDPE Geomembrane Seaming and Vice Versa". Geoynthetics 2019, IFAI, Houston, TX, USA, 10-13 February 2019.

Rowe, R.K., 1988. Contaminant migration through groundwater: the role of modelling in the design of barriers. Can. Geotech. J. 25 (4), 778–798.

Rowe, R.K., 2005. Long-term performance of contaminant barrier systems, 45th Rankine Lecture. Geotechnique 55 (9), 631–678.

Rowe, R.K., 2011. Systems engineering the design and operations of municipal solid waste landfills to minimize leakage of contaminants to groundwater. Geosynth. Int. 16 (6), 391–404.

Rowe, R.K., 2012. Short and long-term leakage through composite liners", the 7th Arthur Casagrande Lecture. Can. Geotech. J. 49 (2), 141–169.

Rowe, R.K., 2018. Environmental geotechnics: looking back, looking forward" (16th Croce Lecture). Italian Geotech. J. (4), 8–40. https://doi.org/10.19199/2018.4.0557-1405.008, 2018.

Rowe, R.K., 2020. Protecting the environment with geosynthetics - the 53rd Karl Terzaghi lecture. ASCE J. Geotech. Geoenviron. Eng. 146 (9), 04020081 https://doi.org/10.1061/(ASCE)GT.1943-5606.0002239.

Rowe, R.K., Booker, J.R., 1995. A finite layer technique for modelling complex landfill history. Can. Geotech. J. 32 (4), 660–676.

Rowe, R.K., Francey, W., 2018. Effect of Dual Track Wedge Welding at 30°C Ambient Temperature on Post-weld Geomembrane Oxidative Induction Time. 11th International Conference on Geosynthetics, Seoul, Korea. September.

Rowe, R.K., Rimal, S., Sangam, H., 2009. Ageing of HDPE geomembrane exposed to air, water and leachate at different temperatures. Geotext. Geomembranes 27 (2), 137–151.

Rowe, R.K., Sangam, H.P., 2002. Durability of HDPE geomembranes. Geotext. Geomembranes 20 (2), 77–95.

Rowe, R.K., Shoaib, M., 2017. Long-term performance of high-density polyethylene (HDPE) geomembrane seams in municipal solid waste (MSW) leachate. Can. Geotech. J. 54 (12), 1623–1636.

Rowe, R.K., Shoaib, M., 2018. Durability of HDPE geomembrane seams immersed in brine for three years. J. Geotech. Geoenviron. Eng. 144 (2), 04017114.

Rowe, R.K., Yu, Y., 2019. Magnitude and significance of tensile strains in geomembrane landfill liners. Geotext. Geomembranes 47 (3), 429–458. https://doi.org/10.1016/j.geotexmem.2019.01.001.

Scheirs, J., 2009. A Guide to Polymeric Geomembranes: a Practical Approach. John Wiley & Sons.

Tuomela, A., Ronkanen, A.-K., Rossi, P.M., Rauhala, A., Haapasalo, H., Kujala, K., 2021. Using geomembrane liners to reduce seepage through the base of tailings ponds—a review and a framework for design guidelines. Geosciences 11 (2), 93.

Zhang, L., Bouazza, A., Rowe, R., Scheirs, J., 2017. Effect of welding parameters on properties of HDPE geomembrane seams. Geosynth. Int. 24 (4), 408–418.